

Contribution

Existing commercial designs for multi-axis force sensors are very expensive, providing a disincentive to their routine and abundant use in human/robot interaction as force sensing handles. While force sensor design has not been a common topic in robotics conferences for several years now, the beginnings of extensive work in human/robot interaction make it a topic worth revisiting.

FORCE SENSORS FOR HUMAN/ROBOT INTERACTION

Andy Lorenz
Michael A. Peshkin
J. Edward Colgate

Department of Mechanical Engineering
Northwestern University
Evanston. IL 60208-3111

Abstract

Conventional force sensors are overdesigned for use in measuring human force inputs, such as is needed in research and application of human/robot interaction. A new type of force sensor is introduced that is suited to human-robot interaction. This sensor is based on optoelectronic measurements rather than strain gauges. Criteria for material selection and dimensioning are given.

1. Introduction

Human-robot interaction is an increasingly important field in robotics. Often this interaction is mediated by a force sensor which is the primary control input for the human. Existing force sensor designs are intended for use at the end effector of a robot to monitor assembly or machining forces. In these applications very high stiffness may be needed. Commercial multi-axis force sensors typically measure all six axes (three forces and three torques).

These requirements are unnecessarily stringent for force sensors to be used in human-robot interaction, and cause force sensors to be so

expensive as to restrict the development of human/robot applications. Since the human hand and arm are so compliant themselves, there is no need for the force sensor itself to be orders of magnitude stiffer.

The force sensor described here is a two axis device designed to measure x-y forces in the plane and to ignore the other four forces and torques. It has far lower stiffness than commercial sensors, allowing approximately one millimeter of deflection at its full scale applied force of 250N. It is simple and inexpensive, using optoelectronic devices in place of strain gauges.

The force sensor can be utilized in human-robot coordination, ([3],[4]) teleoperation ([5]), and collaborative robots ([1],[2]).

2. Benefits of new design

Human-robot interaction requires different properties of a force sensor than typical robot applications such as machining and assembly. These differences have substantial impact on how a force sensor can be designed.

2.1 Larger compliance

Humans are relatively insensitive to small displacements on the order of a millimeter. A force sensor which allows a displacement of this order is not perceptually distinguishable from an ideally stiff one. Millimeter displacements would cause trouble if they occurred at the end effector of a robot, which can be thought of as needing (or benefiting from) the accuracy of a machine tool. So what advantages are obtained by loosening the restrictions on how much displacement is allowed?

Presently, strain gauges are used in most commercially available force sensors. Strain gauges measure the very slight bend of a flexure element caused by applied forces. However, they are difficult to install and calibrate and are easy to break. While the strain gauge elements themselves are inexpensive, in practice their difficulty of application results in sensors costing thousands of dollars.

In the design presented here, infrared LED/photodiode pairs are used as the key sensor element in place of strain gauges. Strain gauges can measure deflections on the order of microns, and so are applied to very stiff flexure elements. Photosensors can be used to measure deflections on the order of millimeters, and thus are applied to much more compliant flexures. Photosensors suffer from some of the same problems as strain gauges, including nonlinearity and temperature sensitivity. However, these sensors have distinct advantages. Photosensors are cheap, easy to mount, are a non-contact sensor, and are hard to break.

In our design, due to properties of the photosensors and the flexure, the axes are intrinsically decoupled; separate sensor elements are used to measure the x and y force components. Since the axes are decoupled, less electronics is needed, and calibration issues are much simpler.

2.2 Fewer degrees of freedom

In an instance where a human controls a robot with fewer than six degrees of freedom, the force sensor need not have six degrees of freedom. Fewer degrees of freedom means a simpler mechanical design, less electronics and wires, fewer sensor elements, and less calibration.

One benefit of the design, which follows partially from having fewer degrees of freedom,

is the resistance of the force sensor to large undesired force components.

For example, consider a person moving a payload suspended from an overhead rail system. Where does one put a force sensor to read the forces applied by the human? If one uses a handle, then the person must grab the device by the handle, even if it might be easier for the person to grasp the payload directly. If one puts the force sensor between the payload and the rail system, then manipulating the object directly is allowed, but the force sensor must withstand the weight of the payload. The type of force sensor presented here would be ideal for this problem, as it can withstand large forces out of the plane to be measured.

3. Design

3.1 Overview

The force sensor is shown in figure 1. The outer mount is the housing, while the handle is connected to the inner piece. Connecting the two pieces is a flexure element, best seen in the upper part of figure 2. The flexure alone is shown in the lower part of figure 2. As forces are applied to the handle, the flexure allows a displacement to occur between the two pieces. Due to the 30:1 (typical) aspect ratio of the flexure, it does not bend significantly in response to forces in the z-direction or torques about the x and y axes.

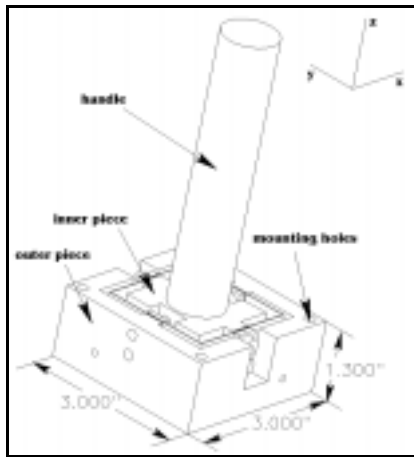


Figure 1

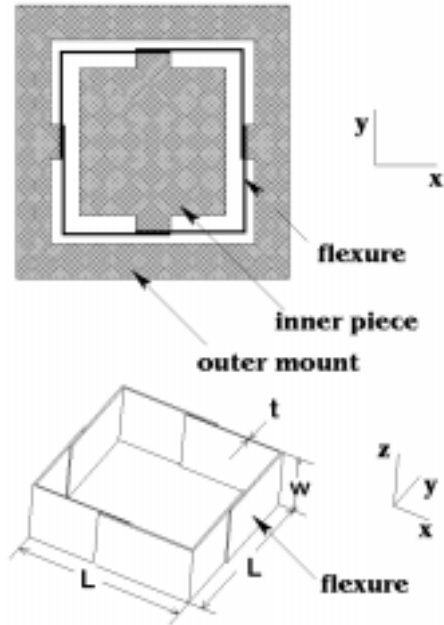


Figure 2

The flexure is designed to withstand one millimeter of motion between the inner and outer pieces, at which point the two pieces physically make contact preventing further motion. This protects the flexure from being broken.

The displacement of the inner piece is measured using infrared “reflective object” sensor elements. These sensor elements are mounted on a printed circuit board which is attached to the inner piece. Each sensor element contains an infrared LED and a photodiode, pointing in the same direction. Light from the LED reflects off the inside wall of the outer piece and is detected by the photodiode, as shown in figure 3.

For each force axis, there are two sensor elements measuring the distance to the two walls of the outer object. The sensor elements labeled A and B in figure 3 for example, are for measuring the x force.

Each pair of sensor elements is incorporated into a circuit shown in figure 4. The output voltage is approximately linearly related to the displacement, for small displacements. For the small deflections discussed here, the displacement is proportional to the force applied..

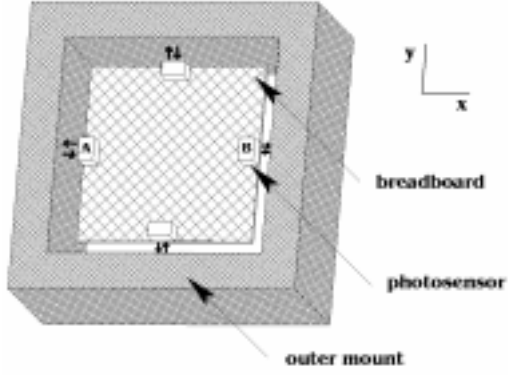


Figure 3

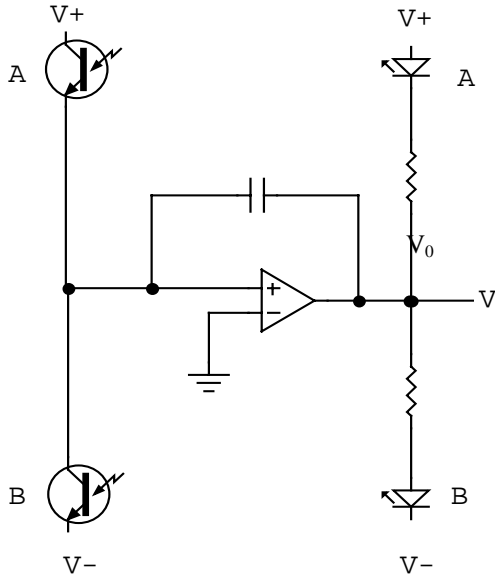


Figure 4

3.2 Compliance matrix

The shape of the flexure can be used to determine its compliance matrix. The flexure can be considered to be constructed of four identical L's (See figure 2). The compliance matrix of these L's is determined, assuming small deflections and simple stress distributions within the cross-section of the beam, as in [7]. The compliance matrix for one L is given below.

$$\underline{A} = \begin{pmatrix} 2 & -\frac{3}{4} & 0 & 0 & 0 & -\frac{9}{4} \\ -\frac{3}{4} & \frac{1}{2} & 0 & 0 & 0 & \frac{3}{4} \\ 0 & 0 & p + \frac{3}{8}k & \frac{3}{4}p + \frac{3}{8}k & -\frac{3}{4}p & 0 \\ 0 & 0 & \frac{3}{4}p + \frac{3}{8}k & \frac{3}{2}p + \frac{3}{8}k & 0 & 0 \\ 0 & 0 & -\frac{3}{4}p & 0 & \frac{3}{2}p + \frac{3}{8}k & 0 \\ -\frac{9}{4} & \frac{3}{4} & 0 & 0 & 0 & 3 \end{pmatrix} \quad (1)$$

$$\Delta \vec{x} \equiv \begin{pmatrix} \Delta x \\ \Delta y \\ \Delta z \\ \Delta \theta_x \\ \Delta \theta_y \\ \Delta \theta_z \end{pmatrix} = \frac{L^3}{Et^3w} \underline{A} \begin{pmatrix} f_x \\ f_y \\ f_z \\ \tau_x \\ \tau_y \\ \tau_z \end{pmatrix} \equiv \frac{L^3}{Et^3w} \underline{A} \vec{f} \quad (2)$$

where $\Delta \vec{x}$ is the displacement, L is the length of one side of the square sheet, E, t, and w are the modulus of elasticity, thickness, and width of the material, $p = t^2/h^2$ is the aspect ratio squared,

$k = \frac{E}{G}$ is the ratio of the modulus of elasticity and the modulus of rigidity of the material, and \vec{f} is the applied force. These compliance matrices are translated and rotated so that they are positioned as in figure 2. Then the compliance matrix of the whole flexure assembly, C, is found by combining the compliances of the individual L's

and the modulus of rigidity of the material, and \vec{f} is the applied force. These compliance matrices are translated and rotated so that they are positioned as in figure 2. Then the compliance matrix of the whole flexure assembly, C, is found by combining the compliances of the individual L's

$$\underline{C} = \left(\sum_i \underline{A}_i^{-1} \right)^{-1} \quad (3)$$

We find that

$$\underline{C} = \begin{pmatrix} \frac{1}{20} & 0 & 0 & 0 & 0 & 0 \\ 0 & \frac{1}{20} & 0 & 0 & 0 & 0 \\ 0 & 0 & p \frac{k+p}{4(k+4p)} & 0 & 0 & 0 \\ 0 & 0 & 0 & p \frac{3(k+p)(k+4p)}{12k^2+80kp+40p^2} & 0 & 0 \\ 0 & 0 & 0 & 0 & p \frac{3(k+p)(k+4p)}{12k^2+80kp+40p^2} & 0 \\ 0 & 0 & 0 & 0 & 0 & \frac{3}{112} \end{pmatrix} \quad (4)$$

$$\Delta \vec{x} = \frac{L^3}{Et^3w} \underline{C} \vec{f}. \quad (5)$$

A number of insights can be gained from this compliance matrix. First, we notice that it is

diagonal, which tells us that forces and torques create only their own corresponding motions. It also tells us how the choice of the aspect ratio (squared) p affects the design. If p is small, then the flexure moves significantly only in response to the forces f_x , f_y , and τ_z . This is how the present design is made. However, if p is large, then we have a flexure that responds to f_z , τ_x , and τ_y . Also we see how the dimensions of the flexure, L , t and w , matter.

3.3 Material selection

The flexure must be able to deflect a desired displacement x_d when the full scale force F is applied in the x (or y) direction. The flexure must not break of fatigue at this deflection. The deflection as a function of force can be obtained from equation 5. It is

$$x_d \equiv \Delta x = \frac{1}{20} \frac{FL^3}{Et^3 w} \quad (6)$$

where $F = f_x$ from equation 1. From a simple materials [7] analysis, we find that the maximum moment M_{\max} , is related to the applied force by

$$M_{\max} = \frac{3}{40} FL \quad (7)$$

The moment of inertia, I , of the flexure when bent about the z -axis is

$$I = \frac{1}{12} wt^3 \quad (8)$$

We want the maximum stress to be a factor of safety less than the yield stress. The equation for the maximum stress is then

$$\sigma_{\max} = \frac{M_{\max} c}{I} = \frac{9}{20} \frac{FL}{wt^2} < \frac{\sigma_y}{F.S.} \quad (9)$$

where $c = t/2$ is the maximum distance from the normal axis of the flexure, σ_y is the yield stress, and $F.S.$ is the factor of safety desired. From equations (6) and (9), we can find equations restricting the length L and thickness t of the material.

$$L < \frac{9}{\sqrt[3]{20}} \frac{(F.S.)x_d^{2/3} F^{1/3} E^{2/3}}{w^{1/3} \sigma_y} \quad (10)$$

$$t = \sqrt[3]{\frac{F}{20x_d E w}} L \quad (11)$$

We want to be able to make a sensor as small as is possible. This implies minimizing L . Thus we should choose a material that will minimize $E^{2/3}/\sigma_y$, or will maximize

$$\frac{\sigma_y^{3/2}}{E}. \quad (12)$$

Certain materials score well by this criteria ([6]). One is high tensile strength steel, such as the “spring steel” we have used. Other high scores are nylon and certain rubbers. The rubbers are probably not feasible, as the thickness, t , would have to be so large as to make the design unreasonable, but nylon or other plastics may be a feasible material. Spring steel has good fatigue properties (when a $F.S.$ of 2 or greater is used), and this may be a problem with plastics. However, spring steel is difficult to machine and bend, as its hardness is similar to that of machine tools and it is rather brittle outside its elastic range.

For spring steel, $F.S.=2$, $y_d=1$ mm, $w=1.9$ cm, $F=66.3$ lb., we find $L_{\min}=4$ cm=1.6 in. This is the value used in the prototype.

3.4 Sensor considerations

As mentioned above, infrared photosensors are used to detect displacement. The arrangement of the sensors in the design are shown in figure 3. One pair of sensors detects motions in the x direction, while the other pair of sensors detects motions in the y direction. The photosensors are reflective, and shine on a uniform reflective flat surface on the outer piece. The sensors detect when the wall comes closer or farther, and are immune to motions parallel with the wall.

This causes the measurements of the two pairs of sensors to be independent, and to measure only their own axis. In addition to this, it causes the sensors to be relatively insensitive to small torques about the z axis. Thus only large z torques that cause range problems for the device

need to be worried about. (Due to the compliance matrix, other unwanted force components, f_z , τ_x , and τ_y , do not have this concern.)

It was found for the photosensor used, QT Optoelectronic's OPB706A reflective sensor, that a decent trade-off between sensitivity and linearity of the sensor response could be obtained if the maximum displacement allowed by the flexure was $\pm 1\text{mm}$.

4. Three-axis force sensor design

Another design for a similar force sensor is shown in figure 5. In this design, there are three pairs of beams in series. An inner piece is attached at the 2 locations labeled B (One is hidden.). An outer piece is attached at the 4 locations labeled A. The heavily shaded beams are thick and do not bend significantly. The beams labeled a, b, and g allow flexing in the x, y and z directions respectively. Each pair of beams allows only motion in one direction. All together this design allows motion only in x, y and z, and allows no twisting of the device. As before, photosensors could be used to measure displacements. There would then be 3 pairs of sensors instead of two.

This design is more complicated. In addition, it lacks some of the compactness of the first design, which can be relatively short in the z direction. However, this design is insensitive to all torques and can withstand large torques without breaking or affecting readings.

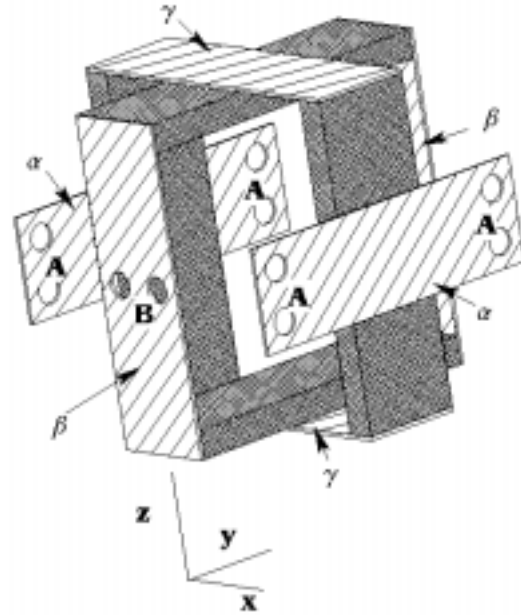


Figure 5

5. Measurements

Linearity, noise, and DC offset drift measurements will be added as soon as completed.

6. Summary

A new force sensor design was described in this paper. It is much cheaper and easier to construct than existing commercial force sensors.

The reduced degrees of freedom (two or three in contrast to six) allows a different class of flexures to be used, two of which are mentioned above. These flexures have a diagonal compliance matrix.

The greater allowable compliance in human/robot applications makes new simpler and cheaper force sensors possible. In addition it allows the use of new types of sensors.

The force sensor described above allows measurement of forces in a plane. It is insensitive to other force components. These force components do not significantly bend the flexure, thus they do not have to be measured and then cancelled. The designs can be modified so that these force components can be very large, and still not break or significantly bend the flexure.

The combination of this class of flexures and photosensors allows the axes to be orthogonal, simplifying sensor placement, electrical design, and calibration.

REFERENCES

- [1] J. E. Colgate, W. Wannasuphprasit, and M. A. Peshkin, "Cobots: Robots for Collaboration with Human Operators," Proc. 1996 ASME Int. ME Cong. and Exhib., Atlanta, GA, DSC-Vol. 58, pp. 433-39.
- [2] W. Wannasuphprasit, R. B. Gillespie, J. E. Colgate, M. A. Peshkin, "Cobot Control," Proc. 1997 IEEE Int. Conf. on R&A, Albuquerque, NM, pp. 3571-3577.
- [3] O. M. Al-Jarrah and Y. F. Zheng, "Arm-Manipulator Coordination for Load Sharing Using Compliant Control," Proc 1996 Int. Conf on R&A, Columbus, OH, pp. 1000-1005.
- [4] K. I. Kim and Y. F. Zheng, "Human-robot Coordination with Rotational Motion," Proc. 1998 IEEE Int. Conf. on R&A, Leuven, Belgium, pp. 3480-3485.
- [5] A.K. Bejczy and Z.F. Szakaly, "A harmonic motion generator(HMG) for telerobotic applications," Proc. 1991 IEEE Int. Conf. on R&A, Sacramento, CA, 1991, pp. 2032-2039.
- [6] M.F. Ashby, "Material Property Charts" ASM Handbook Vol. 20, pg. 266-280, ASM International, 1997.
- [7] F. P. Beer and E. R. Johnston, Jr., Mechanics of Materials, McGraw-Hill, 1976